

Supplementary Materials for  
***P*-type dye-sensitized solar cells based on pseudorotaxane  
mediated charge-transfer**

Tessel Bouwens,<sup>a</sup> Simon Mathew<sup>a</sup> and Joost N. H. Reek\*<sup>a</sup>

<sup>a</sup> Homogeneous, Supramolecular and Bio-Inspired Catalysis, Van 't Hoff Institute for Molecular Sciences  
University of Amsterdam  
Science Park 904, 1098XH Amsterdam (The Netherlands)

Email: [j.n.h.reek@uva.nl](mailto:j.n.h.reek@uva.nl)

## Contents

1. $^1\text{H}$ NMR and $^{13}\text{C}$ NMR of <b>1</b> and <b>P<sub>N</sub></b>	3
2. IR compound <b>1</b> , <b>P<sub>N</sub></b> and IR of <b>P<sub>N</sub>@NiO</b>	7
3. CV and DPV of <b>P<sub>N</sub></b> , <b>P1</b> , <b>RING<sup>4+</sup></b> and <b>MV<sup>2+</sup></b>	10
4. Fluorescence binding study	15
5. NMR study on <b>P<sub>N</sub></b> -ring complexation	16
6. Excited state quenching study	18
7. I-V curve	19
8. DSSC with varying <b>RING<sup>4+</sup></b> concentration	20
9. Dye coverage	22
10. References	23



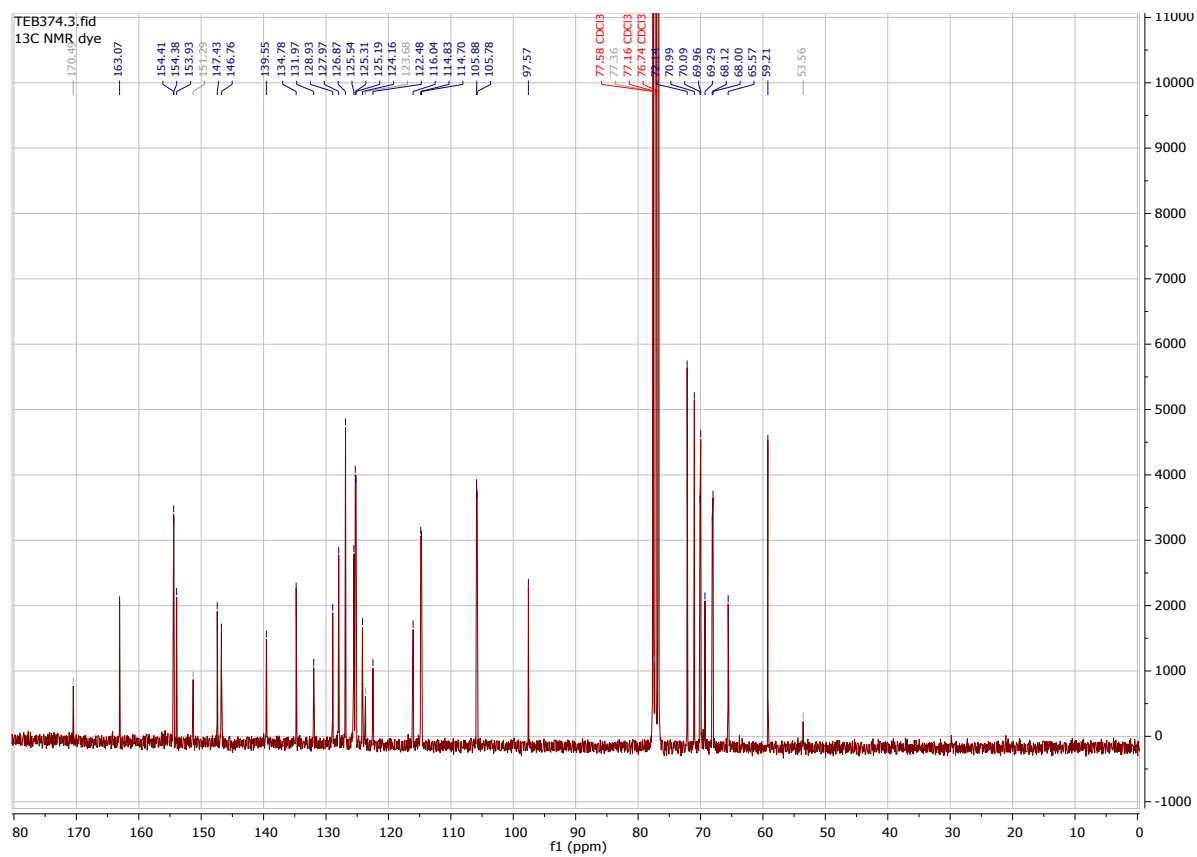


Figure S2: <sup>13</sup>C NMR (300 MHz, 298 K) of the final product  $P_N$  in  $CDCl_3$ .

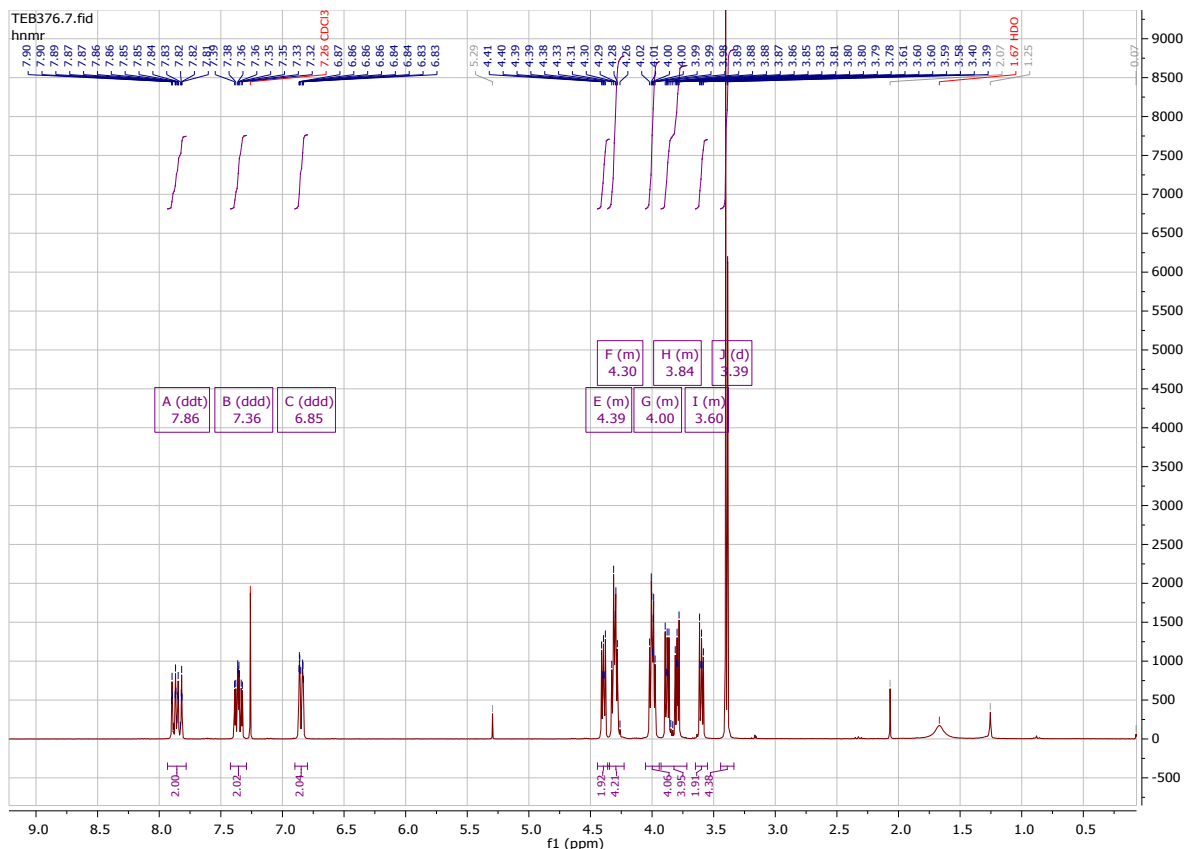


Figure S3:  $^1\text{H-NMR}$  (300 MHz, 298 K) of compound **1** in  $\text{CDCl}_3$ .

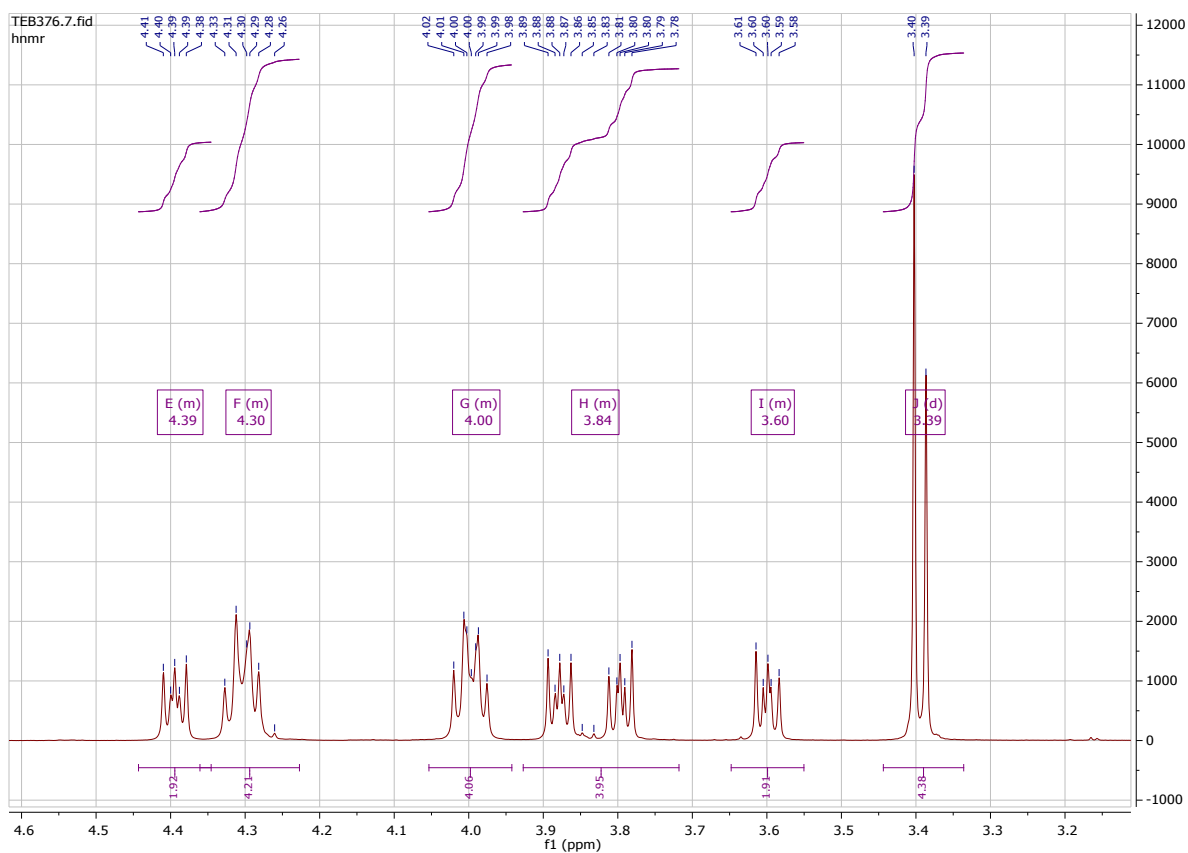


Figure S4:  $^1\text{H-NMR}$  (300 MHz, 298 K) of compound **1** in  $\text{CDCl}_3$  zoom from 4.6 ppm to 3.2 ppm.

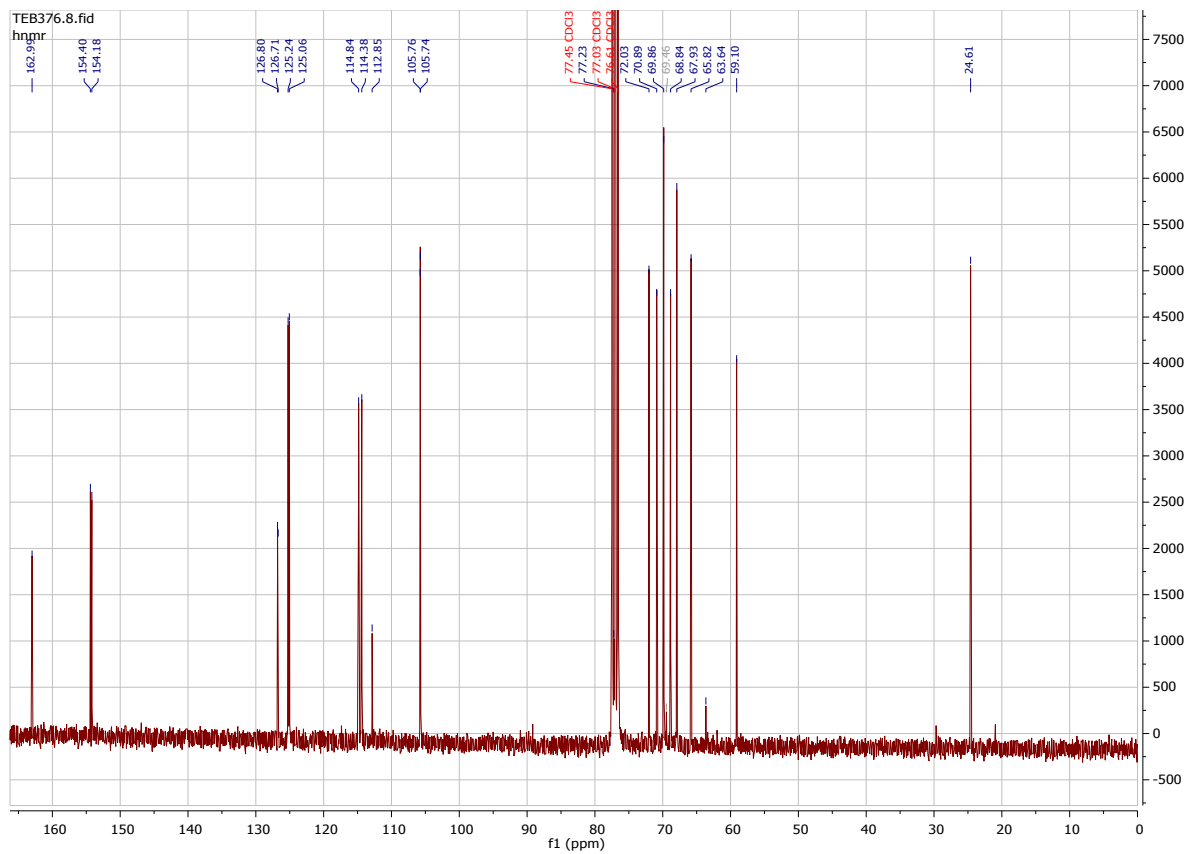


Figure S5:  $^{13}\text{C-NMR}$  (300 MHz, 298 K) of compound **1** in  $\text{CDCl}_3$ .

## 2. IR compound 1, $P_N$ and IR of $P_N@NiO$

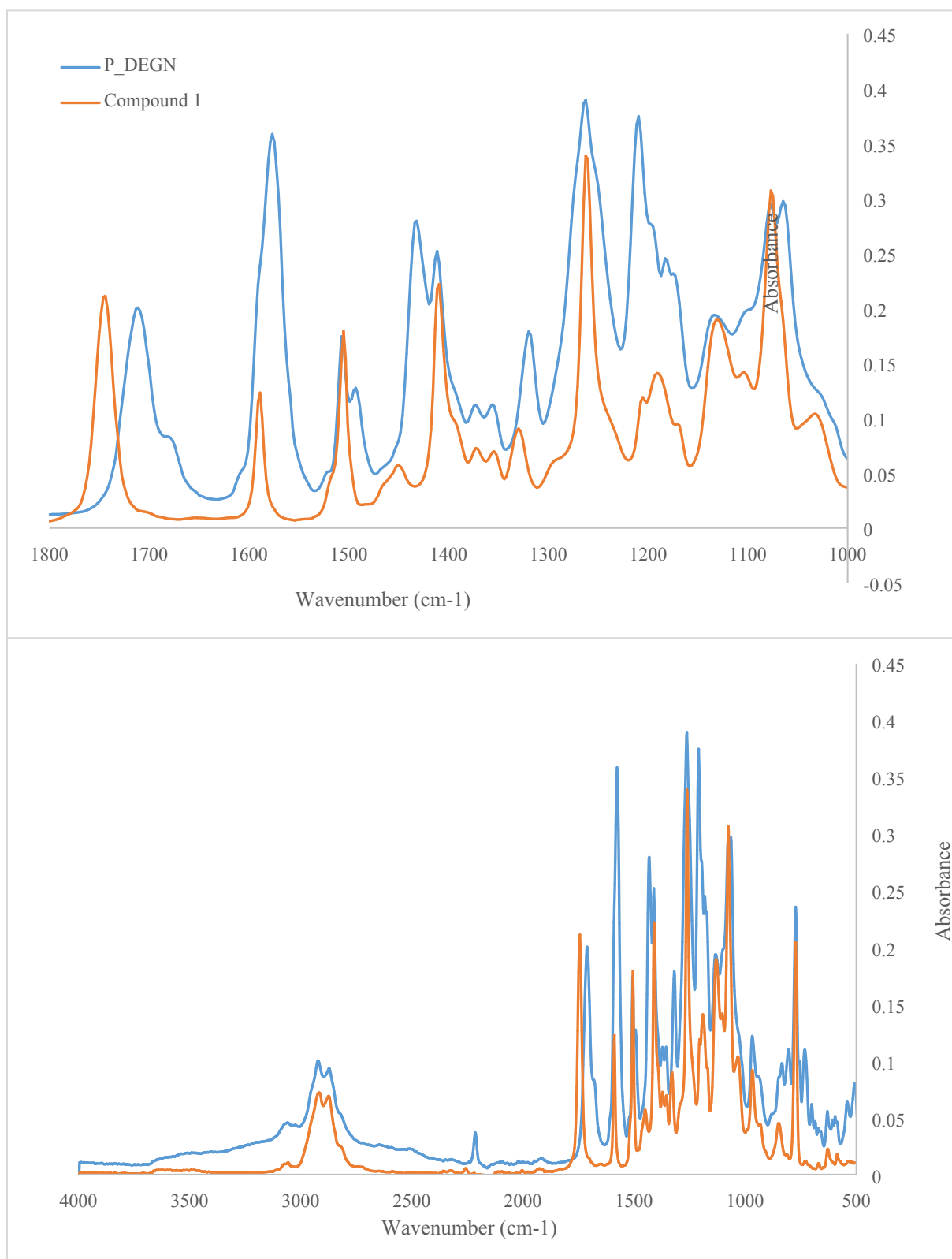


Figure S6: IR spectrum of  $P_N$  (blue) and compound **1** (orange) (bottom) and zoom-in of IR spectrum (top). The C=O stretch in compound **1** is blue shifted compared to  $P_N$ .  $P_N$  contains two different C=O stretch signals: one from the ester functionality and one originates from the conjugated acid which is visible as a weaker shoulder peak next to 1713 cm<sup>-1</sup>.

Table S1: IR absorptions and Interpretation for compound 1.

Absorption (cm <sup>-1</sup> )	Appearance	Interpretation
3060	br	OH (COOH)
2924	m	CH <sub>2</sub> (ethylene glycol)
2226	w	CN
1749	s	C=O (ester)

Table S2: IR absorptions and Interpretation for compound P<sub>N</sub>.

Absorption	Appearance	Interpretation
3061	br	OH (COOH)
2924	m	CH <sub>2</sub> (ethylene glycol)
2217	w	CN
1713	s	C=O (ester)
1680	m	C=O (COOH)

### Dye adsorption onto NiO

Figure S8 shows the ATR-IR spectrum of the P<sub>N</sub> dye and of the P<sub>N</sub> dye adsorbed onto NiO. In this spectrum the carbonyl region shows two signals that can be assigned to the ester carbonyl (at 1730 cm<sup>-1</sup>) and of the of the acidic carboxyl group at 1680 cm<sup>-1</sup> (see Figure S7). Upon adsorption the ν<sub>C=O</sub> band of the acidic group of the dye at 1680 cm<sup>-1</sup> is lost as can be seen in the spectrum (grey line). This indicates that the dye is indeed chemisorbed to the NiO surface via the carboxyl group.

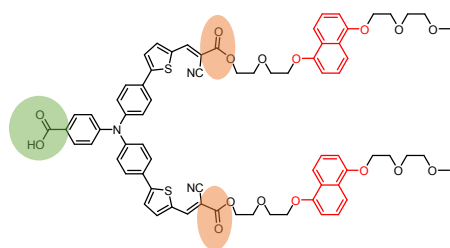


Figure S7: The structure of P<sub>N</sub> with the carbonyl groups highlighted of the ester (orange) and of the carboxylic acid (green)

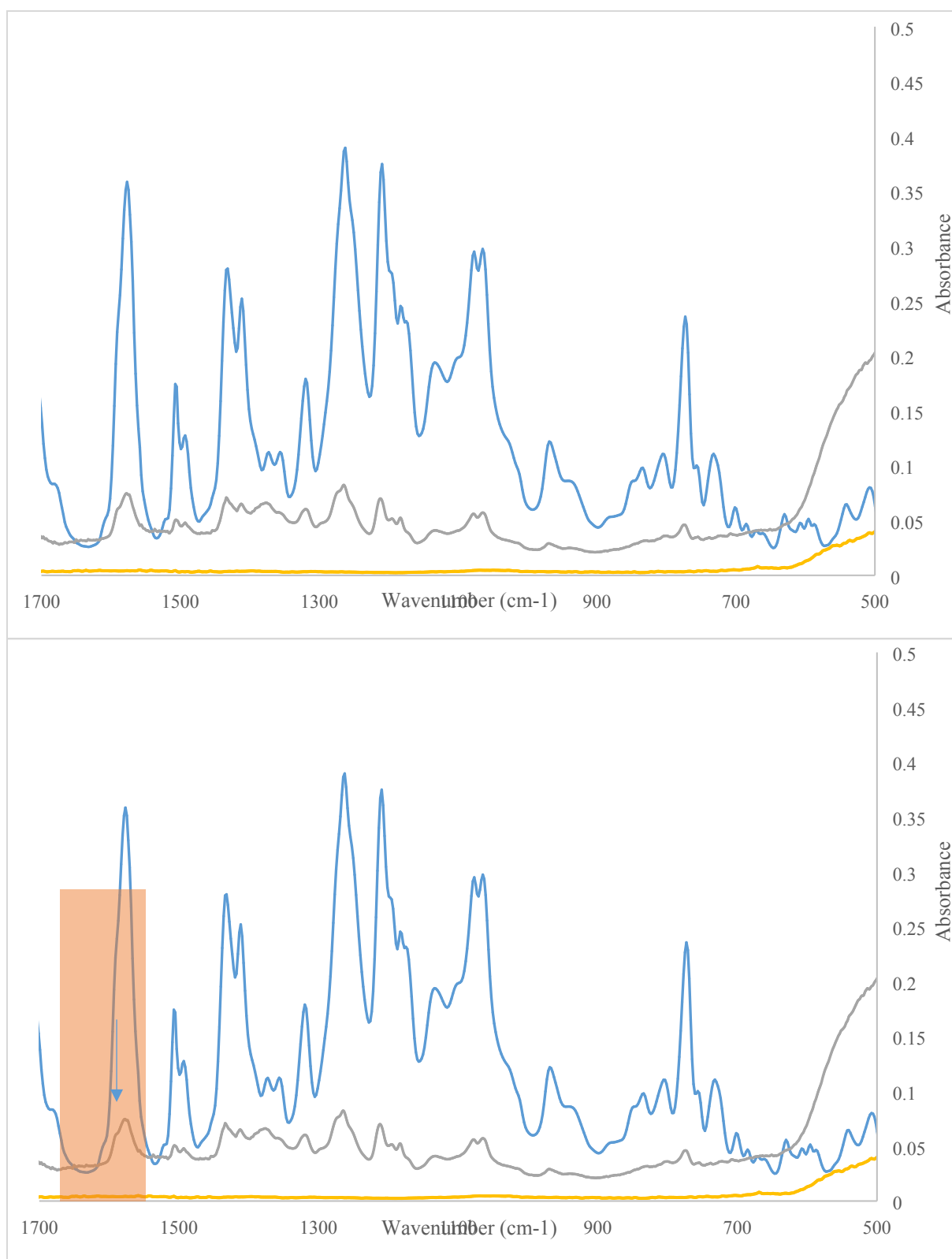


Figure S8: IR spectrum of  $P_N$  (blue),  $P_N$  adsorbed onto NiO (grey), and NiO (yellow) (top) and zoom in of IR spectrum (bottom) with the C=O stretch vibration highlighted. The arrow points to the C=O stretch vibration that originates from the conjugated acid (COOH) that is absent when  $P_N$  is adsorbed onto NiO.

### 3. CV and DPV of $P_N$ and $P_1$ , $RING^{4+}$ and $MV^{2+}$ $P_1$

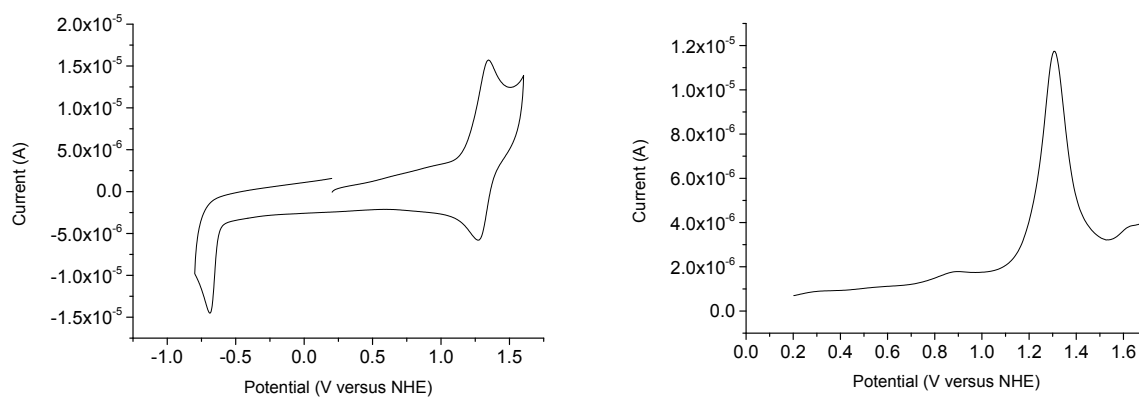


Figure S9: Cyclic voltammogram of  $P_1$  start from 0.2 V, upper limit at 1.6 V and lower limit at -0.8 V with scan rate  $0.1 \text{ V s}^{-1}$  (left) and differential pulse voltammogram measured from 0 to 1.7 V (right) in 0.1 M  $TBAPF_6$  in MeCN using glassy carbon as working electrode, leakless Ag/AgCl as reference electrode and Pt-wire as counter electrode.

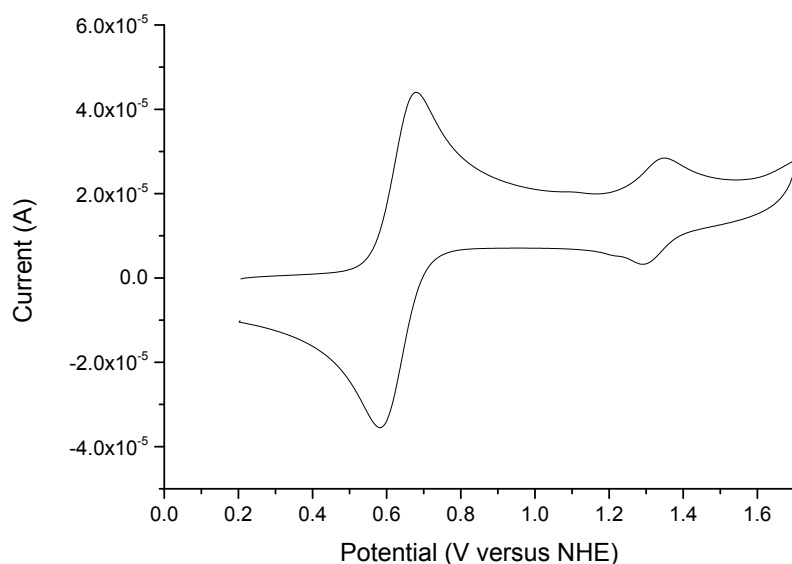


Figure S10: Cyclic voltammogram of  $P_1$  start from 0.2 V, upper limit at 1.7 V with scan rate  $0.1 \text{ V s}^{-1}$  in presence of ferrocene (first wave) in 0.1 M  $TBAPF_6$  in MeCN using glassy carbon as working electrode, leakless Ag/AgCl as reference electrode and Pt-wire as counter electrode.

In order to determine the position of the redox waves, ferrocene was added as a redox standard. Since it is known that the ferrocene couple has a potential of 630 mV versus NHE, the redox potentials of the  $P_1$  and the  $P_N$  dye could be determined versus NHE.<sup>1</sup> The reported electrochemical properties in Table 1 are determined from these voltammograms.

**P<sub>N</sub>**

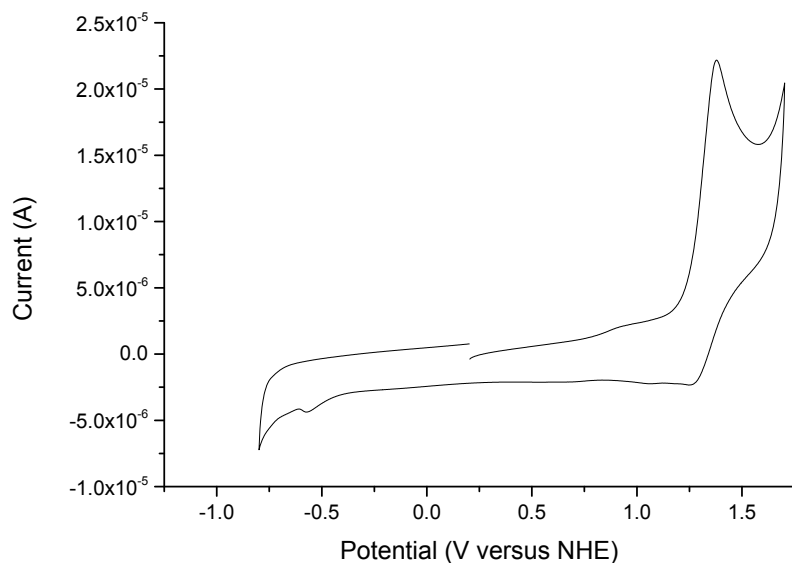


Figure S11: Cyclic voltammogram of P<sub>N</sub> start from 0.2 V, upper limit at 1.6 V and lower limit at -0.8 V with scan rate 0.1 V s<sup>-1</sup> in 0.1 M TBAPF<sub>6</sub> in MeCN using glassy carbon as working electrode, leakless Ag/AgCl as reference electrode and Pt-wire as counter electrode.

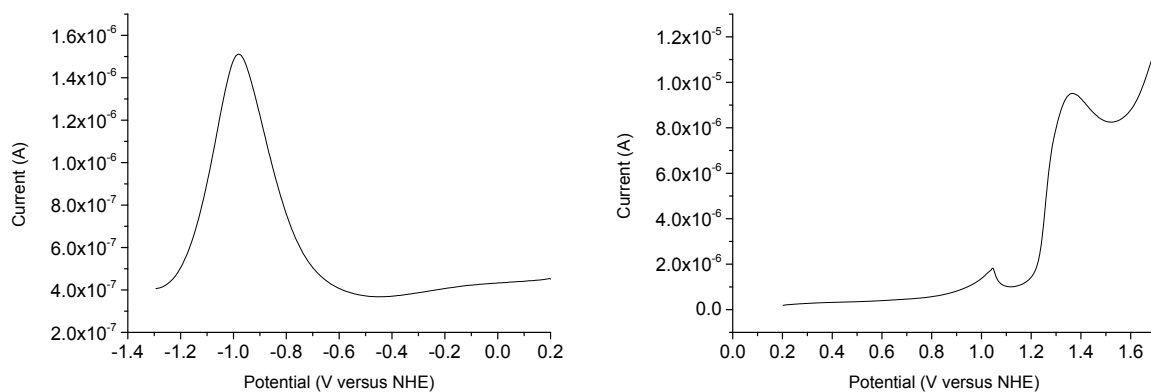


Figure S12: Differential pulse voltammogram of P<sub>N</sub> measured from 0 to -1.3 (left) and from 0 to 1.7 V (right) using glassy carbon as working electrode, leakless Ag/AgCl as reference electrode and Pt-wire as counter electrode.

### **MV<sup>2+</sup>** and RING<sup>4+</sup>

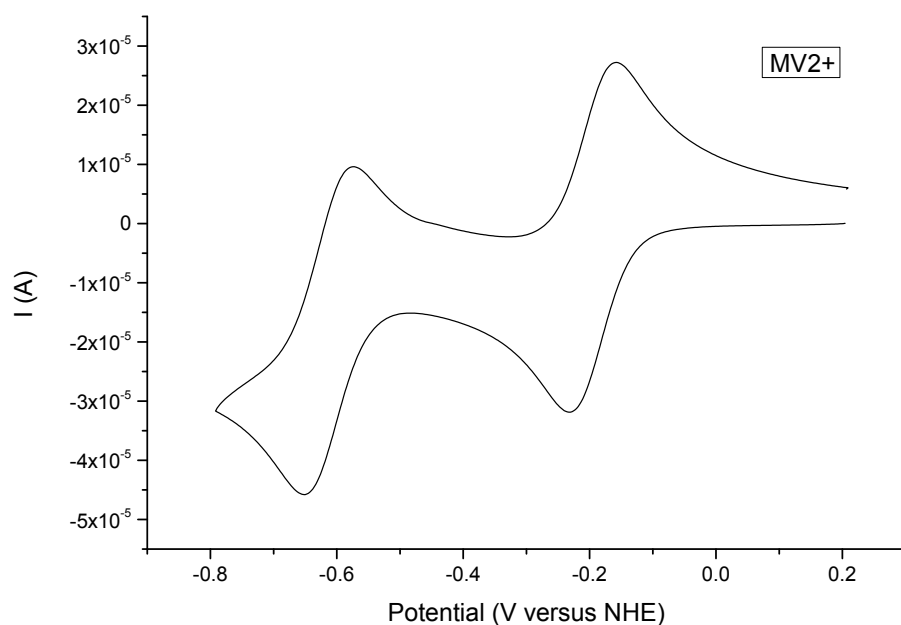


Figure S13: Cyclic voltammogram of **MV<sup>2+</sup>** start from 0.2 V, upper limit at 0.2 V and lower limit at -0.8 V with scan rate 0.1 V s<sup>-1</sup> in 0.1 M TBAPF<sub>6</sub> in MeCN using glassy carbon as working electrode, leakless Ag/AgCl as reference electrode and Pt-wire as counter electrode.

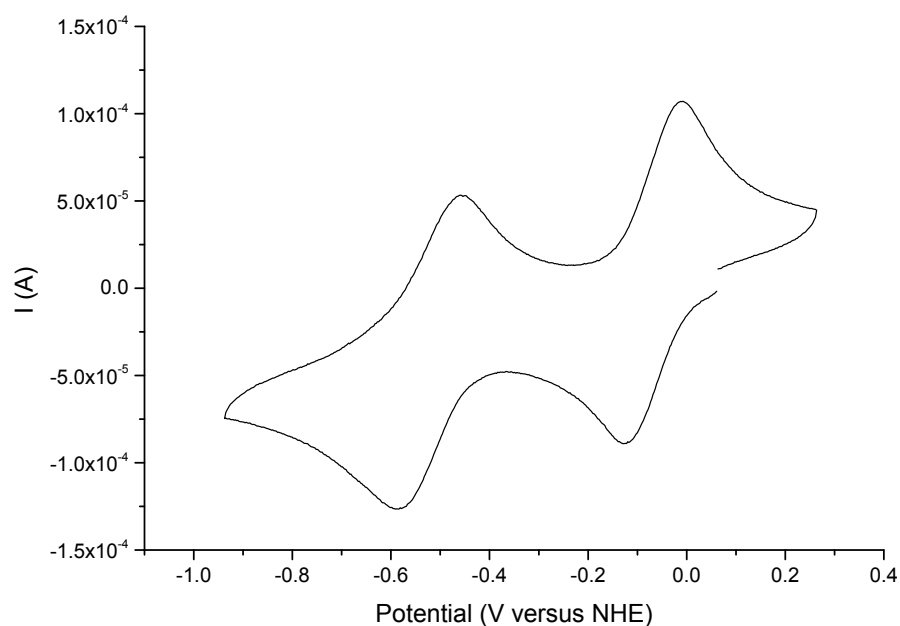


Figure S14: Cyclic voltammogram of **RING<sup>4+</sup>** start from 0.05 V, upper limit at 0.2 V and lower limit at -0.9 V with scan rate 0.1 V s<sup>-1</sup> in 0.1 M TBAPF<sub>6</sub> in MeCN using glassy carbon as working electrode, leakless Ag/AgCl as reference electrode and Pt-wire as counter electrode.

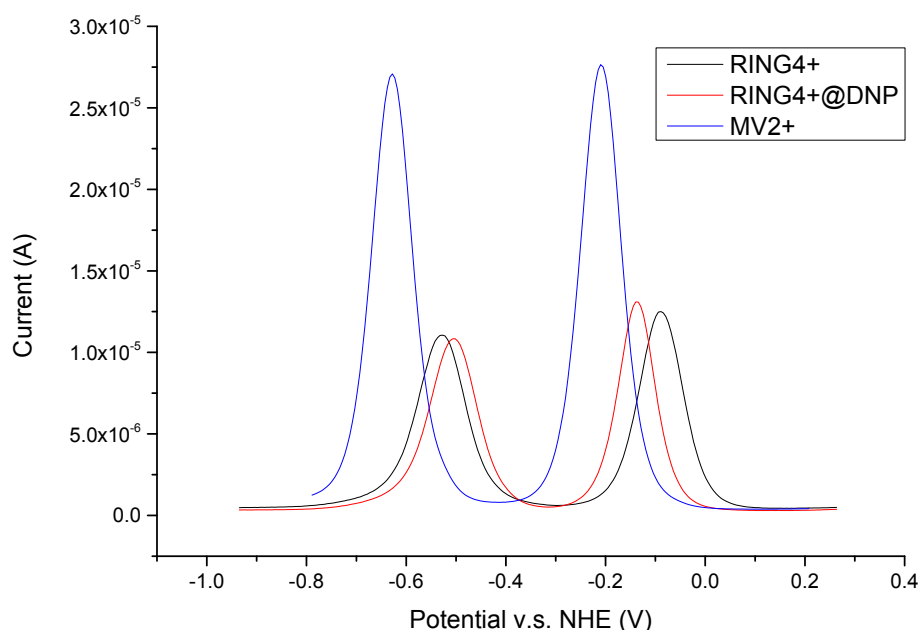


Figure S15: Differential Pulse Voltammogram of **RING<sup>4+</sup>** (black) **MV<sup>2+</sup>** (blue) and **RING<sup>4+</sup>** with DNP (red) start from 0.3 V and lower limit at -0.95 V with scan rate 0.005 V s<sup>-1</sup> in 0.1 M TBAPF<sub>6</sub> in MeCN using glassy carbon as working electrode, leakless Ag/AgCl as reference electrode and Pt-wire as counter electrode.

Table S3:  $E_{1/2}$  determined from CV and DPV of **MV<sup>2+</sup>**, **RING<sup>4+</sup>** and **RING<sup>4+/2+</sup>@DNP**.

Compound	Reduction potential $E_{1/2}$ (V versus NHE)
<b>MV<sup>2+/+•</sup></b>	-209
<b>RING<sup>4+/2+•</sup></b>	-78.9
<b>RING<sup>4+/2+•</sup>@DNP</b>	-134

The cyclic voltammograms of **MV<sup>2+</sup>** and **RING<sup>4+</sup>** are shown in Figure S13 and Figure S14 respectively. The voltammogram of **MV<sup>2+</sup>** is characterized by two reversible waves of which the first wave corresponds to the **MV<sup>2+/+•</sup>** redox couple and the second wave corresponds to the **MV<sup>+•/0</sup>** transition. In case of the ring, two separate waves are observed as well, however both waves are characterized by a two electron reduction since there are two identical MV units present in this molecule as was established by Stoddart and coworkers.<sup>2</sup> The first wave is assigned to the **RING<sup>4+/2+•</sup>** couple and the second wave corresponds to the two electron reduction of **RING<sup>2+•</sup>** to the neutral **RING<sup>0</sup>**. This means that electrochemically the **RING<sup>3+•</sup>** cannot be observed, however, photochemically this oxidation state is accessible since this is a one electron process.

The observed  $E_{1/2}$  values are summarized in Table S3. This shows that for the first reduction of **MV<sup>2+/+•</sup>** the  $E_{1/2}$  is at a more negative potential than the  $E_{1/2}$  of **RING<sup>4+/2+•</sup>**. Figure 6 shows the recorded Differential Pulse Voltammograms in which an overlap region is visible between reduction peaks of **MV<sup>2+</sup>** and **RING<sup>4+</sup>** indicating that reduction of **MV<sup>2+</sup>** by the ring is indeed possible. Interestingly, the  $E_{1/2}$  of **RING<sup>4+/2+•</sup>** becomes more negative when it is associated to DNP by approximately 50 mV. Although DSSC are not at equilibrium we can estimate how much **RING<sup>3+</sup>** can reduce **MV<sup>2+</sup>** using the Nernst equation at equilibrium.<sup>3</sup>

If we consider the following reaction:



The ratio between  $\text{RING}^{4+}/\text{RING}^{3+}$  can be determined with

$$\text{Log} \frac{\text{RING}^{4+}}{\text{RING}^{3+}} = 8.47 \Delta E^{\circ}$$

$$\text{This gives us } \frac{\text{RING}^{4+}}{\text{RING}^{3+}} = 0.08$$

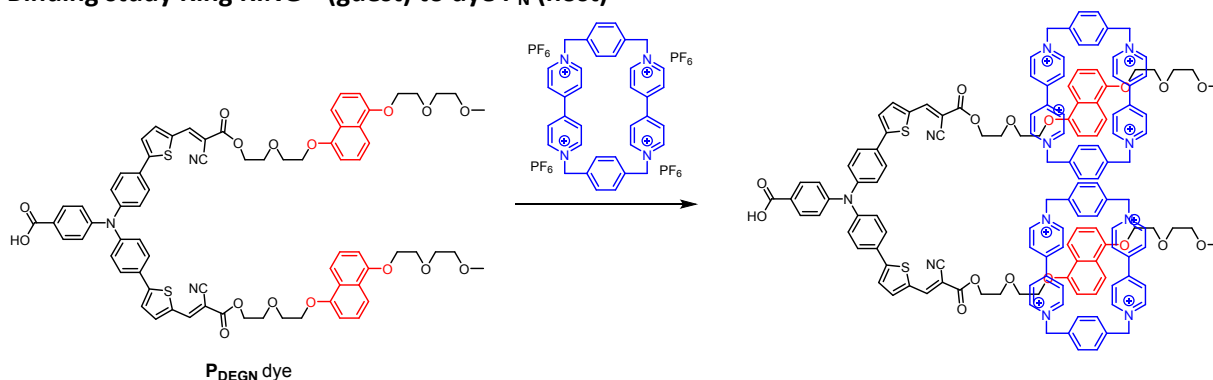
$$0.08 \cdot 75 \mu\text{M} = 6 \mu\text{M}$$

$$K_{\text{eq}} = \frac{[\text{RING}^{4+}][\text{MV}^{+•}]}{[\text{RING}^{3+}][\text{MV}^{2+}]}$$

$K_{\text{eq}}$  is then found to be 12.6

## 4. Fluorescence binding study

Binding study Ring RING<sup>4+</sup> (guest) to dye P<sub>N</sub> (host)



Fit with HGG system. Binding constant  $K_{ass}$  found  $6.3E4$  and  $\alpha=0.7$

Corrected I @ 310 nm

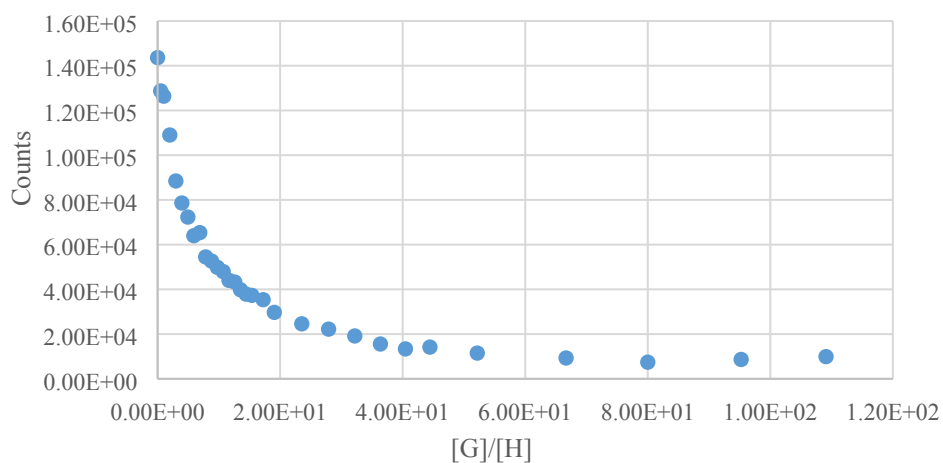


Figure S16: Corrected fluorescence quenching of P<sub>N</sub> naphthyl fluorescence at 344 nm upon excitation at 310 nm by addition of ring to determine the binding constant  $K_{ass}$ .

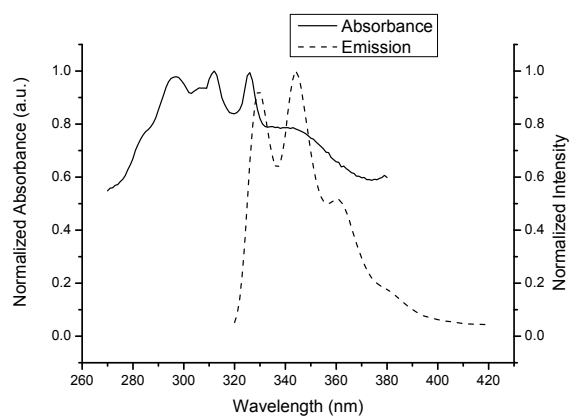


Figure S17: The absorbance of the DNP unit in P<sub>N</sub> (solid line) and its structured fluorescence (dotted line).

## 5. NMR studies on P<sub>N</sub>-ring complexation

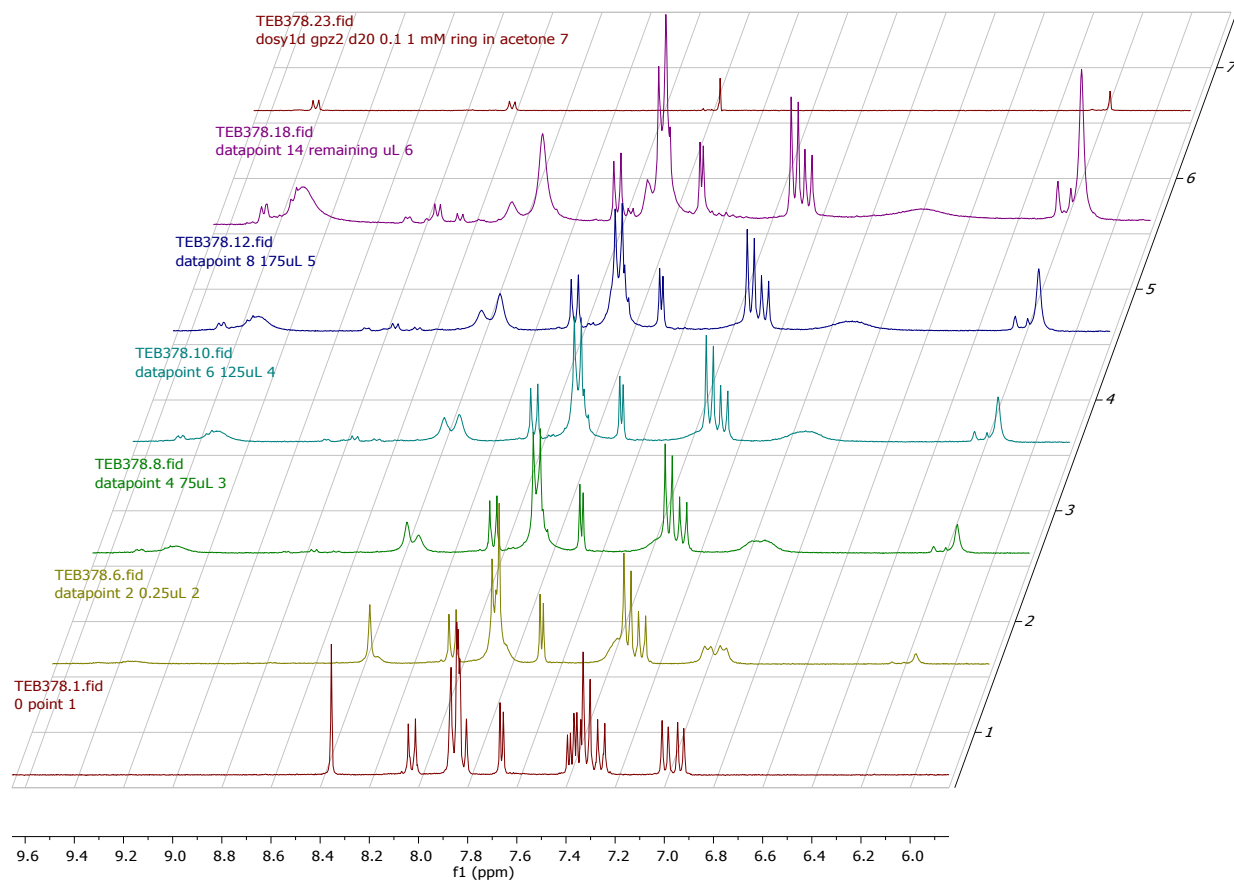


Figure S18: Apparent NMR shift and broadening of the signals of the P<sub>N</sub> dye upon addition of ring in (CD<sub>3</sub>)<sub>2</sub>CO. Spectrum 1 shows spectrum before addition of ring and spectrum 6 with 5 equivalents of ring. The naphthyl proton signals at 6.9 ppm broaden and shift to 6.6 ppm. The NMR shifts of unbound ring in d-acetone are represented in spectrum 7.

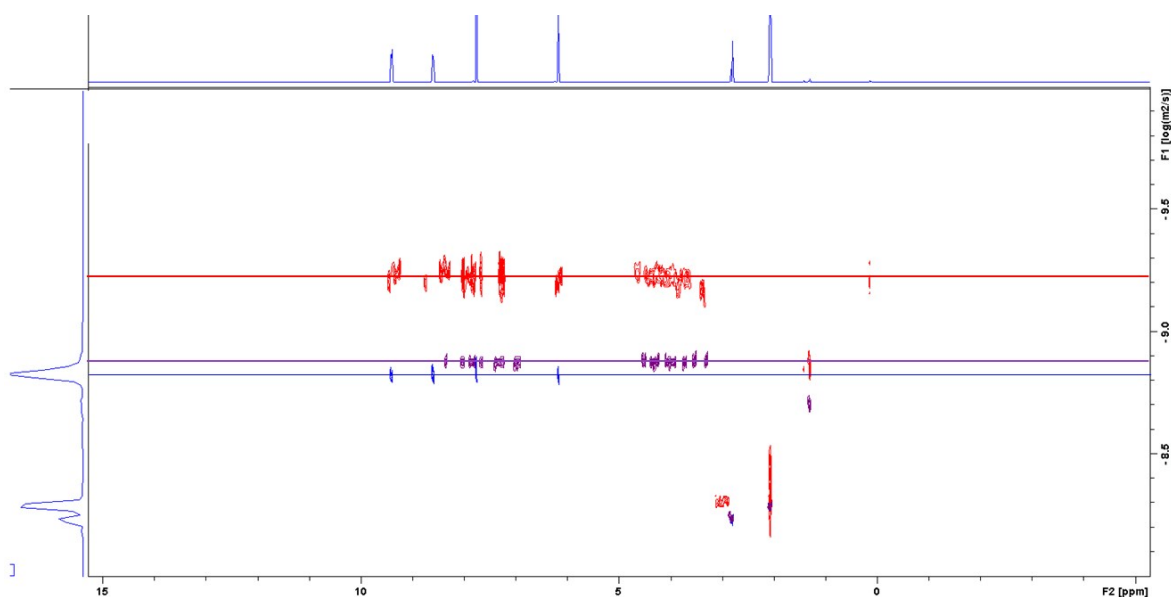


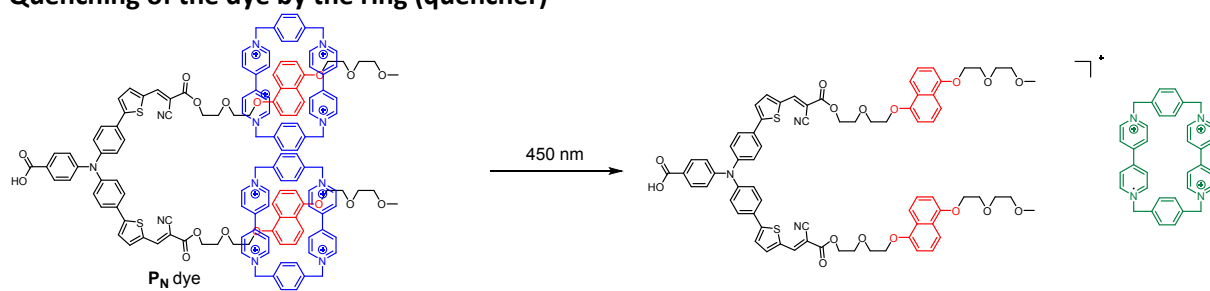
Figure S19: DOSY spectra of free  $P_N$  dye (purple), free ring  $RING^{4+}$  (blue) and of the pseudorotaxane, complexed ring to  $P_N$  dye. Since the ring and dye signals are on the same line, they have diffusion coefficient and therefore this belongs to the same species, namely the pseudorotaxane.

Table S4: Apparent diffusion coefficient derived from the DOSY data and their calculated radius. The radius was determined via the Stokes-Einstein equation.

	$P_N$	$RING^{4+}$	$P_N-(RING^{4+})_2$
-LogD	8.99	8.90	9.26
D ( $m^2 s^{-1}$ )	1.02E-9	1.26E-9	5.50E-10
Radius (nm)	0.7	0.7	1.3

## 6. Excited State quenching study

### Quenching of the dye by the ring (quencher)



I (340 nm)

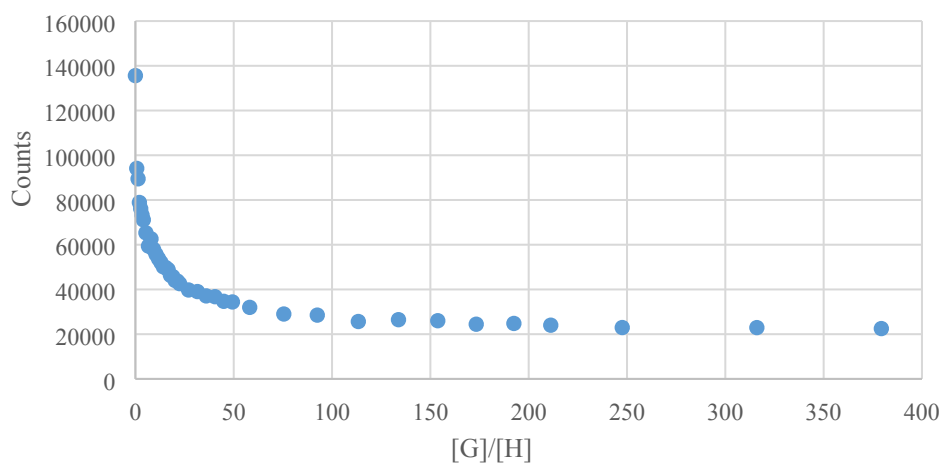


Figure S20: Fluorescence quenching of the excited state of  $P_N$  at 630 nm upon excitation at 450 nm by addition of  $RING^{4+}$  (quencher).

## 7. I-V curve $P_N$ 0.3% ring and MV

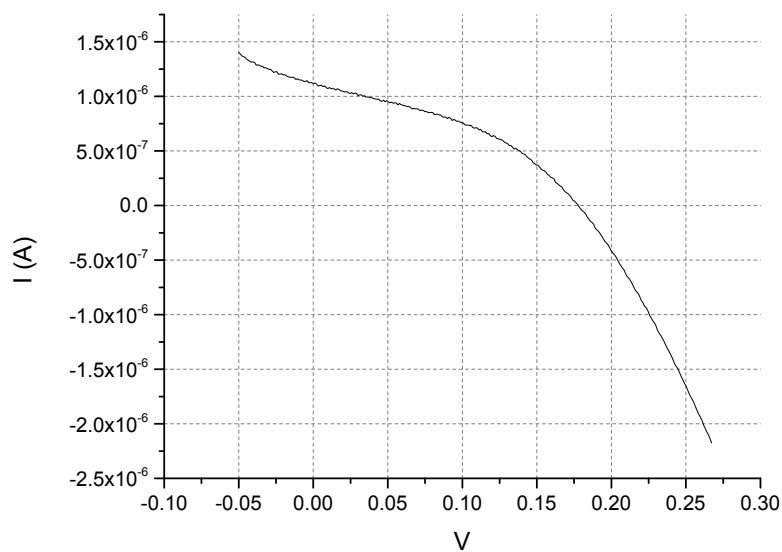


Figure S21: I-V curve for the DSSCs constructed of the  $P_N$  dye and the 0.3% ring in 25 mM MV electrolyte.

Table S5: Solar cell results for the DSSCs constructed of the  $P_N$  dye and the 0.3 mol%  $RING^{4+/3+}$  in 25 mM  $MV^{2+/+}$  electrolyte.  $V_{oc}$  = open-circuit voltage;  $I_{sc}$  = short-circuit current; FF= fill factor;  $P_{in}$  is the power put into the system ( $W m^{-2}$ );  $P_{max}$  is the maximum power generated by the cell ( $W m^{-2}$ );  $\eta$ =power conversion efficiency as %.

$V_{oc}$	$I_{sc}$	$V_{mp}$	$I_{mp}$	FF	$P_{in}$	$P_{max}$	$\eta(\%)$
1.79E-01	1.12E-06	0.112305	6.99E-07	3.91E-01	0.023562	0.023562	3.33E-04

## 8. DSSC with varying RING<sup>4+</sup> concentration

### Cells in absence of MV<sup>2+</sup>

DSSC in absence of MV<sup>2+</sup> with Ring (75 μM) in 1 M LiTFSI was prepared with MeCN inside a nitrogen filled glovebox as is described in the experimental section.

The photovoltaic results are shown in Figure S22. In case of **P1** a very small negative photocurrent density is observed of 0.26 μA cm<sup>-2</sup> which is 4 times smaller than the current densities that are observed for the RING<sup>4+</sup> MV<sup>2+</sup> mix in the **P1** cell and 40 times smaller than the best performing **P<sub>N</sub>** cell. This lower current is due to low electrolyte concentration, (75 μM ring in this case instead of 25 mM MV<sup>2+</sup> with 0.3% ring).

In case of the cell consisting of **P<sub>N</sub>** positive photocurrents are observed. This most likely due to capacitor effects rather than the solar cell function. When this cell is irradiated for a longer period of time, the positive current preserves on decreasing indicating that capacitance is built up (Figure 23). As there are  $1.61 \times 10^{-8}$  mol cm<sup>-2</sup> dye molecules on the NiO, our cell contains 3.1 nmol dye and only 0.32 nmol RING<sup>4+/3+</sup> under the conditions applied (see SI 9 for this determination). As the  $K_{\text{ass}}$  is high for ring to the DNP unit, most of the rings will be associated to the dye molecules at the surface as we have a 10 times excess of dye. Effectively there is no redox mediator and therefore the excited dye injects its electron in the NiO trap states rather than the redox mediator for which a positive current is observed.

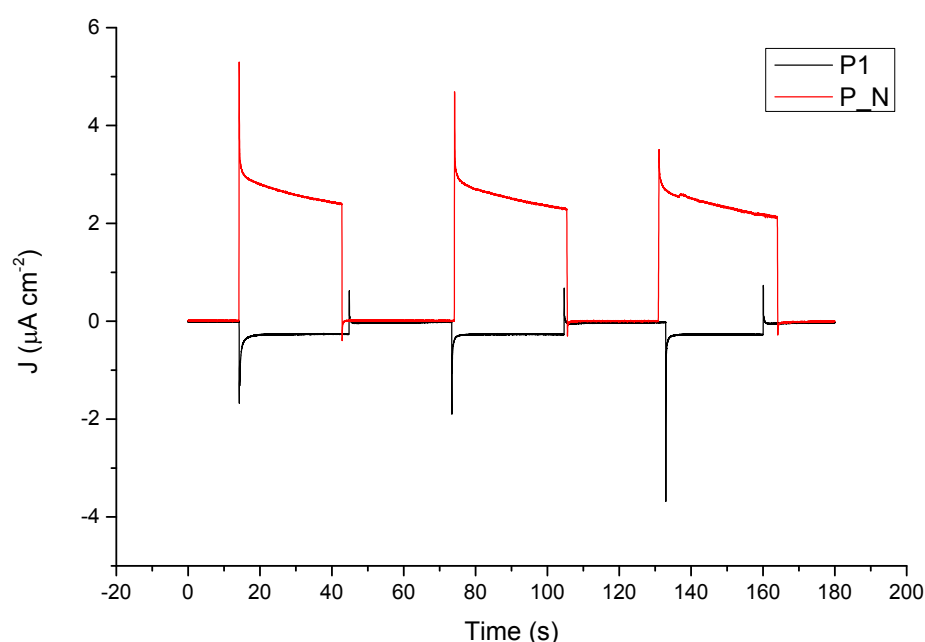


Figure S22: Observed photocurrent densities upon irradiation of the DSSC containing 75 μM RING<sup>4+/3+</sup> in 1 M LiTFSI for **P1** (black line) and **P<sub>N</sub>** (red line).

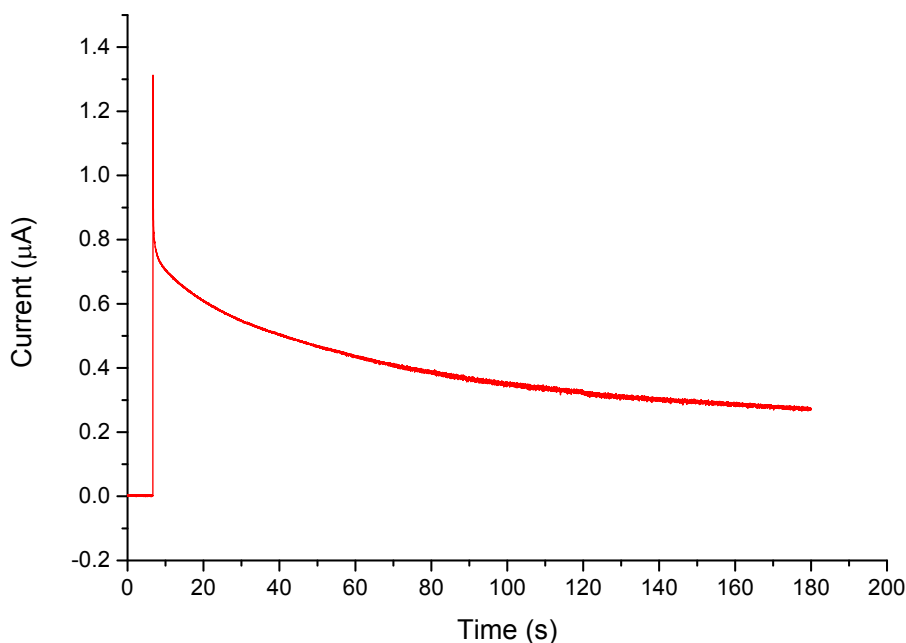


Figure S23: Decrease of photocurrent observed for DSSC containing  $P_N$  as a dye with  $75 \mu\text{M RING}^{4+/3+}$  in  $1 \text{ M LiTFSI}$ .

From these experiments it becomes clear that the presence of  $MV^{2+}$  is essential for the DSSC to function.

If  $RING^{4+}$  concentration is increased, the dye leaches. Photocurrents that can be measured are extremely low in this case. The figure below gives an example of a chronoamperometry measurement with 5%  $RING^{4+}$ . Dye leach is observed as soon as the electrolyte is introduced into the cell with concentration above 1%.

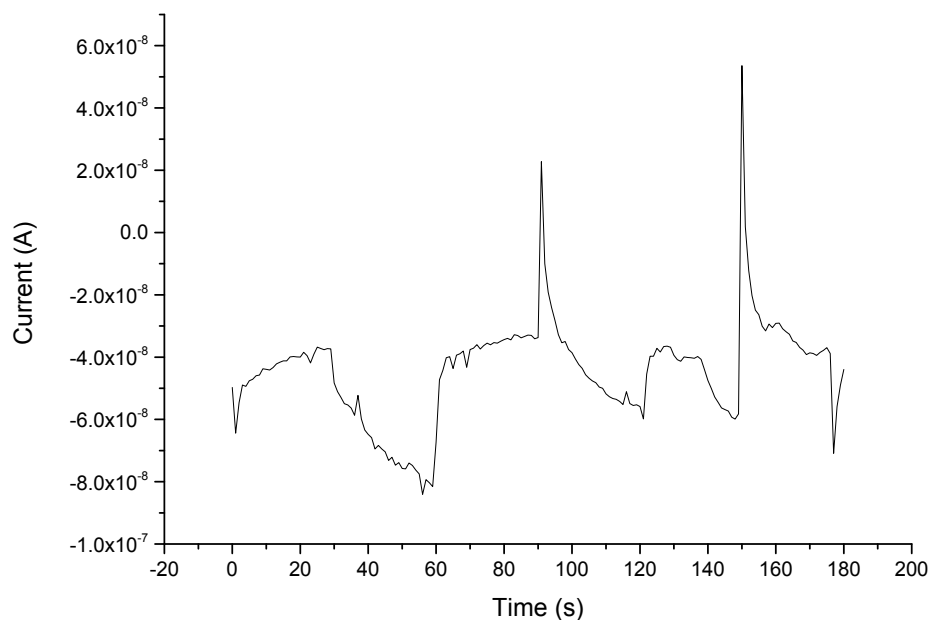


Figure S24: Observed photocurrent densities upon irradiation of the DSSC containing 5% ( $1.25 \text{ mM}$ )  $RING^{4+/3+}$  in  $24.75 \text{ mM MV}^{2+/+}$  with  $1 \text{ M LiTFSI}$  supporting electrolyte in case of  $P_N$  dye.

## 9. Dye coverage

The dye coverage on NiO was determined by dye desorption. Since experiments using base (TBAOH) led to complete dye decomposition and acid treatment did not lead to full desorption, a concentrated solution of **RING**<sup>4+</sup> was used (20 mM, 10 mL) to induce dye leach. The sensitized electrode was sonicated for 30 minutes. From this mixture 5 mL was centrifuged. From this, 2 mL was used to record the UV absorption. The amount of dye was determined via the extinction coefficient using Lambert-Beer law.

$$A(\lambda) = \epsilon \cdot c \cdot l$$

Using this approach it was determined that the dye coverage is  $1.61 \times 10^{-8} \text{ mol cm}^{-2}$ .

Completion of dye desorption was confirmed as no orange color was observed at the NiO.

## 10. References

- 1 V. V. Pavlishchuk and A. W. Addison, *Inorganica Chim. Acta*, 2000, **298**, 97–102.
- 2 P. L. Anelli, P. R. Ashton, D. Philp, M. Pietraszkiewicz, M. V. Reddington, N. Spencer, J. F. Stoddart, C. Vicent, R. Ballardini, V. Balzani, M. T. Gandolfi, L. Prodi, M. Delgado, T. T. Goodnow, A. E. Kaifer, A. M. Z. Slawin and D. J. Williams, *J. Am. Chem. Soc.*, 1992, **114**, 193–218.
- 3 N. G. Connelly and W. E. Geiger, *Chem. Rev.*, 1996, **96**, 877–910.